

A physics-compliant *diagonal* representation for wireless channels parametrized by *beyond-diagonal* reconfigurable intelligent surfaces

Philipp del Hougne, *Member, IEEE*

Abstract—The parametrization of wireless channels by so-called “beyond-diagonal reconfigurable intelligent surfaces” (BD-RIS) is mathematically characterized by a matrix whose off-diagonal entries are partially or fully populated. Physically, this corresponds to tunable coupling mechanisms between the RIS elements that originate from the RIS control circuit. Here, we derive a physics-compliant *diagonal* representation for BD-RIS-parametrized channels. Recognizing that the RIS control circuit, irrespective of its detailed architecture, can always be represented as a multi-port network with auxiliary ports terminated by tunable individual loads, we physics-compliantly express the BD-RIS-parametrized channel as a multi-port chain cascade of *i*) radio environment, *ii*) static parts of the control circuit, and *iii*) individually tunable loads. Thus, the cascade of the former two systems is terminated by a system that is mathematically always characterized by a diagonal matrix. This physics-compliant diagonal representation implies that existing algorithms for channel estimation and optimization for conventional (“diagonal”) RIS can be readily applied to BD-RIS scenarios. We demonstrate this in an experimentally grounded case study. Importantly, we highlight that, operationally, an ambiguous characterization of the cascade of radio environment and the static parts of the control circuit is required, but not the breakdown into the characteristics of its two constituent systems nor the lifting of the ambiguities. Nonetheless, we demonstrate how to derive or estimate the characteristics of the static parts of the control circuit for pedagogical purposes. The diagonal representation of BD-RIS-parametrized channels also enables their treatment with coupled-dipole-based models like PhysFad. In passing, we furthermore derive the assumptions under which the physics-compliant BD-RIS model for generic (potentially rich-scattering) radio environments simplifies to the widespread linear cascaded model.

Index Terms—Beyond-diagonal reconfigurable intelligent surface, physics-compliant channel model, multi-port network theory, multi-port chain cascade, end-to-end physics-compliant channel estimation, ambiguity, PhysFad.

I. INTRODUCTION

The properties of the channels used for wireless communications are traditionally imposed by the preexisting radio environment. With the advent of the “smart radio environment” [2]–[6], the wireless channels become to some extent controllable because they are deterministically parametrized by so-called reconfigurable intelligent surfaces (RISs) that are placed within the radio environment. An RIS

is an array of elements with individually adjustable scattering properties. In practise, an RIS often takes the form of an array of patch antennas, each terminated by an individually tunable load impedance. Both in simplified cascaded channel models as well as in physics-compliant end-to-end channel models, the tunable RIS configuration appears along the diagonal of an otherwise empty matrix (see details in Sec. II below). For this reason, we refer to such conventional RIS designs as “diagonal RIS” (D-RIS) in this paper.

To further increase the RIS-based control over the wireless channels without increasing the number of RIS elements, it has been proposed to go beyond D-RIS with RIS designs whose tunability is mathematically represented by more densely (potentially fully) populated matrices, again both in simplified cascaded models and physics-compliant models (see details in Sec. II below) [7], [8]. Following the terminology put forth in Refs. [7], [8], we refer to such RIS designs as “beyond-diagonal RIS” (BD-RIS) in this paper. Physically, these non-zero off-diagonal terms correspond to *controllable coupling effects between RIS elements that originate from the RIS load circuit* as opposed to *uncontrollable mutual coupling via the radio environment due to proximity and reverberation*. Indeed, any physics-compliant model involves potentially significant but uncontrollable interactions between the RIS elements via the radio environment but these are hence qualitatively different from the tunable interactions via the load circuit proposed in BD-RIS.¹

A wide range of designs of the tunable coupling mechanisms between RIS elements in BD-RIS is theoretically conceivable; Refs. [7], [8] provide a taxonomy of carefully crafted designs ranging from pair-wise tunable couplings to all-to-all tunable couplings. To date, their experimental realization remains largely an open challenge and, to the best of our knowledge, only tunable load networks allowing for neighbor-to-neighbor couplings were experimentally realized in conceptually equivalent contexts of RFID channel estimation [15] and contactless scattering matrix estimation with a “virtual vector network analyzer” [16]. Incidentally, a simple-to-realize alternative coupling design that has not received any attention to date would be random tunable

Parts of this work were presented at the 25th IEEE International Workshop on Signal Processing Advances in Wireless Communications (SPAWC) 2024 [1].

P. del Hougne is with Univ Rennes, CNRS, IETR - UMR 6164, F-35000 Rennes, France (e-mail: philipp.del-hougne@univ-rennes.fr).

¹The concepts of “non-local metasurfaces” and “non-local metamaterials” studied in other communities relate to various mechanisms for carefully designed but typically static coupling between meta-atoms [9]–[11]. Although in some experimental realizations of reverberation-non-local metasurfaces the meta-atoms are individually programmable [12]–[14], these hence do not constitute realizations of the BD-RIS concept.

couplings, implemented, for instance, via a tunable chaotic cavity backing the RIS.

In this paper, we introduce a thus far overlooked and at first sight counter-intuitive perspective on the representation of BD-RIS-parametrized wireless channels. Specifically, we propose a physics-compliant end-to-end representation of BD-RIS-parametrized wireless channels involving a *diagonal* tunable matrix. Our fundamental insight is that irrespective of the BD-RIS load circuit design, the latter is itself a multi-port network partially terminated by tunable individual loads. Hence, the BD-RIS-parametrized wireless channel is a multi-port chain cascade of three systems:

- i) the radio environment,
- ii) the static parts of the load circuit (from here on referred to as load circuit for conciseness), and
- iii) the individual tunable loads.

The conventional approach considers the radio environment whose auxiliary ports associated with the RIS elements are terminated by the cascade of load circuit and individual tunable loads that is characterized by a “beyond diagonal” matrix. Our alternative approach considers the cascade of radio environment with load circuit; the auxiliary ports of this cascade associated with tunable lumped elements within the load circuit are then terminated by individual tunable loads that are characterized by a diagonal matrix.

The most important implication of our formulation from a signal-processing perspective is that, in principle, our formulation obviates the need to develop new algorithms for BD-RIS, be it for end-to-end channel estimation or to optimize the BD-RIS configuration; instead, existing algorithms for D-RIS can be directly applied to BD-RIS by replacing the radio environment with the cascade of radio environment and load circuit. Note that for any practical realization of a BD-RIS, the characteristics of the load circuit will necessarily be well defined and hence known or characterizable.

A. Contributions

The contributions of the present paper are summarized as follows:

- 1) *Physics-compliant diagonal representation of BD-RIS-parametrized channels.* We provide a physics-compliant end-to-end formulation in terms of scattering parameters that is more compact than the formulation in terms of impedance parameters that we proposed in the associated conference paper [1] because the wireless channel matrix is an off-diagonal block of a scattering matrix (see Sec. II). Moreover, the scattering-parameter formulation can be applied to canonical BD-RIS load circuit designs for which an impedance or admittance formulation would fail.
- 2) *Identification of assumptions necessary to derive simplified cascaded model from physics-compliant model.* We clarify the assumptions under which one can derive the widespread simplified cascaded channel model for BD-RIS from the fully physics-compliant end-to-end channel model based on multi-port network theory. Previously, only the assumptions under which one can

derive the cascaded model for D-RIS based on PhysFad were elaborated in Ref. [17].

- 3) *Identification of the load circuit scattering matrix \mathbf{S}^{LC} .* We analytically derive \mathbf{S}^{LC} for load circuits based on ideal T or π networks with tunable impedances. We also explain how \mathbf{S}^{LC} can be obtained numerically in a single full-wave simulation given a concrete practical load circuit, as well as why it cannot be estimated experimentally without ambiguities and why that does not pose any problem.
- 4) *Experimentally grounded demonstration of physics-compliant end-to-end estimation and optimization of BD-RIS-parametrized channels using D-RIS algorithms.* We demonstrate in an experimentally grounded case study that D-RIS algorithms for channel estimation and optimization can be readily applied to BD-RIS-parametrized channels. We use scattering measurements obtained within a complex experimental environment and consider that the RIS elements are connected in groups of two to ideal π networks whose impedances can take two possible values corresponding to those of a commercial PIN diode. To the best of our knowledge, this is the first experimentally grounded study on BD-RIS. We demonstrate that we can estimate the parameters of the proposed physics-compliant diagonal representation such that we can subsequently maximize the received signal strength indicator (RSSI) of a single-input single-output (SISO) link. We highlight ambiguities in the estimated parameters and demonstrate that, operationally, they do not matter. Importantly, we only characterize the cascade of radio environment and load circuit, without ever breaking it down into its two constituents. In other words, determining \mathbf{S}^{LC} is in fact not required (except for pedagogical reasons in the previous point).
- 5) *Treatment of BD-RIS within coupled-dipole-based physics-compliant channel models like PhysFad [18], [19].* We clarify that the proposed physics-compliant diagonal representation also answers the open question of how coupled-dipole-based models can cope with the BD-RIS concept. The dipoles represent the primary entities, which are the transmitter and receiver ports as well as the tunable lumped elements. The dipoles are coupled to each other via background Green’s functions lumping together complex scattering in the environment (including structural scattering) in the D-RIS case and, capturing the scattering within the cascade of the radio environment and the load circuit in the BD-RIS case.

B. Outline

The remainder of this paper is organized as follows. In Sec. II, we develop the physics-compliant multi-port network chain cascade description of BD-RIS-parametrized wireless channels, free of any approximations, that yields the diagonal representation at the core of this paper. In Sec. III, we identify the scattering properties of the load circuit analytically for two canonical ideal load circuits, and we discuss how to determine it numerically or experimentally for practical load

circuits. In Sec. IV, we demonstrate the direct applicability of existing channel estimation and optimization algorithms for D-RIS in an experimentally grounded case study of a BD-RIS-parametrized rich-scattering SISO link. In Sec. VI, we briefly conclude.

C. Notation

- The superscripts T , $*$ and \dagger and denote the transpose, the conjugate and the transpose conjugate, respectively.
- \mathbf{I}_d denotes the $d \times d$ identity matrix.
- $\mathbf{0}_d$ denotes the $d \times d$ zero matrix.
- $\text{diag}(\mathbf{a})$ denotes the matrix whose diagonal entries are those of the vector \mathbf{a} and all other entries are zero.

II. THEORY

The generic multi-port chain cascade formulation for BD-RIS-parametrized wireless channels developed in this section is based on multi-port network theory which can equivalently be expressed in terms of scattering, impedance or admittance parameters. We use scattering parameters in this section for two reasons: first, scattering parameters yield a more compact formulation since the wireless channels are scattering coefficients; second, scattering parameters are suitable to describe canonical examples of BD-RIS load circuits that constitute pathological special cases in which impedance parameters cannot be defined. The general impedance formulation can be found in our associated conference paper [1]. A discussion about the relation to equivalent coupled-dipole-based physics-compliant channel formulations like PhysFad [17]–[20] is provided in Sec. V.

Throughout this paper, we assume that the discussed ports and auxiliary ports are monomodal. Otherwise, extensions of the presented theory in terms of generalized scattering parameters [21] would be required. We further make the common and typically applicable assumptions that the considered multi-port networks are linear, passive, time-invariant and reciprocal. We make no assumptions or approximations beyond those stated in this paragraph.

A. Problem statement

Building on a decade-old circuit theory of communication [22], [23], the literature contains by now many proposed formulations for physics-inspired models of D-RIS-parametrized channels based on multi-port network theory [7], [24]–[36], as well as three formulations for BD-RIS-parametrized channels [1], [16], [37]. These numerous formulations differ regarding the approximations and assumptions that they make, especially regarding the nature of the radio environment. In the present paper, we do not make any assumptions beyond those stated in the previous paragraph, ensuring that our formulation is fully physics-compliant. Moreover, we work with the most compact and universal multi-port description of an arbitrarily complex smart radio environment that describes the latter with the scattering matrix $\mathbf{S}^{\text{RE}} \in \mathbb{C}^{N_{\text{RE}} \times N_{\text{RE}}}$ that lumps together all scattering effects, including scattering objects and walls

(irrespective of whether they are point-like or not) and structural scattering [38]–[40] by antennas and RIS elements. Importantly, the number of parameters is hence independent of the radio environment’s complexity and only depends on the number of attached ports $N_{\text{RE}} = N_{\text{T}} + N_{\text{R}} + N_{\text{S}}$, where N_{T} , N_{R} and N_{S} denote the number of transmitting antennas, receiving antennas and RIS elements, respectively. Moreover, as long as \mathbf{S}^{RE} is known or can be estimated², no explicit description of the radio environment (in terms of geometry, materials, etc.) is necessary. These two important aspects first emerged in PhysFad-based works [19], [20] and were subsequently transposed to an equivalent multi-port network formulation in Ref. [28] where all required model parameters were extracted from a single full-wave simulation for an overwhelmingly complicated D-RIS-parametrized on-chip radio environment featuring reflective walls, extended dielectric layers and strong structural scattering.

The N_{S} auxiliary ports associated with the N_{S} RIS elements are terminated by a tunable load circuit. Irrespective of the detailed design of this load circuit (we study a few canonical examples in Sec. III-A), it is clear that the load circuit is parametrized by N_{C} tunable lumped elements: hence, the load circuit must be amenable to a description as a multi-port network with $N_{\text{LC}} = N_{\text{S}} + N_{\text{C}}$ ports, of which N_{S} are connected to the radio environment’s RIS elements and N_{C} are terminated by individual tunable loads. This is the key insight underpinning the present paper that was thus far overlooked in the BD-RIS literature. A D-RIS is a special case of this generic description in which $N_{\text{S}} = N_{\text{C}}$ and the load circuit takes the trivial form of connecting each RIS element auxiliary port directly and uniquely to one tunable lumped element. Mathematically, we thus have $\mathbf{S}^{\text{LC}} = [\mathbf{0}_{N_{\text{S}}} \quad \mathbf{I}_{N_{\text{S}}}; \mathbf{I}_{N_{\text{S}}} \quad \mathbf{0}_{N_{\text{S}}}]$ in the case of a D-RIS.

Overall, as illustrated in Fig. 1, the BD-RIS-parametrized radio environment is hence a chain cascade of radio environment (RE), load circuit (LC), and individual tunable loads (IL). To work out the end-to-end wireless channel matrix $\mathbf{H} \in \mathbb{C}^{N_{\text{R}} \times N_{\text{T}}}$, we can proceed in two distinct manners. As shown in Fig. 1, the conventional perspective (albeit never explicated in this manner so far) first evaluates the cascade of LC and IL, yielding a *generally “beyond-diagonal”* scattering matrix that terminates the radio environment’s auxiliary ports associated with the RIS elements. The alternative perspective, highlighted and leveraged in the present paper, first cascades RE and LC, which yields a multi-port network whose auxiliary ports associated with the tunable lumped elements are then terminated by IL which is characterized by a scattering matrix that is *always diagonal*. We elaborate on these two perspectives in the subsequent subsections.

B. Conventional perspective

As mentioned, for the conventional perspective, we begin by evaluating the cascade of LC and IL that is characterized by

²See Ref. [16], [19], [30] for various experimentally realized methods for end-to-end channel estimation, with varying degrees of parameter ambiguities. Irrespective of these ambiguities, the end-to-end wireless channels are correctly predicted as a function of D-RIS configuration in all cases. Further discussion is provided in Sec. IV-B.

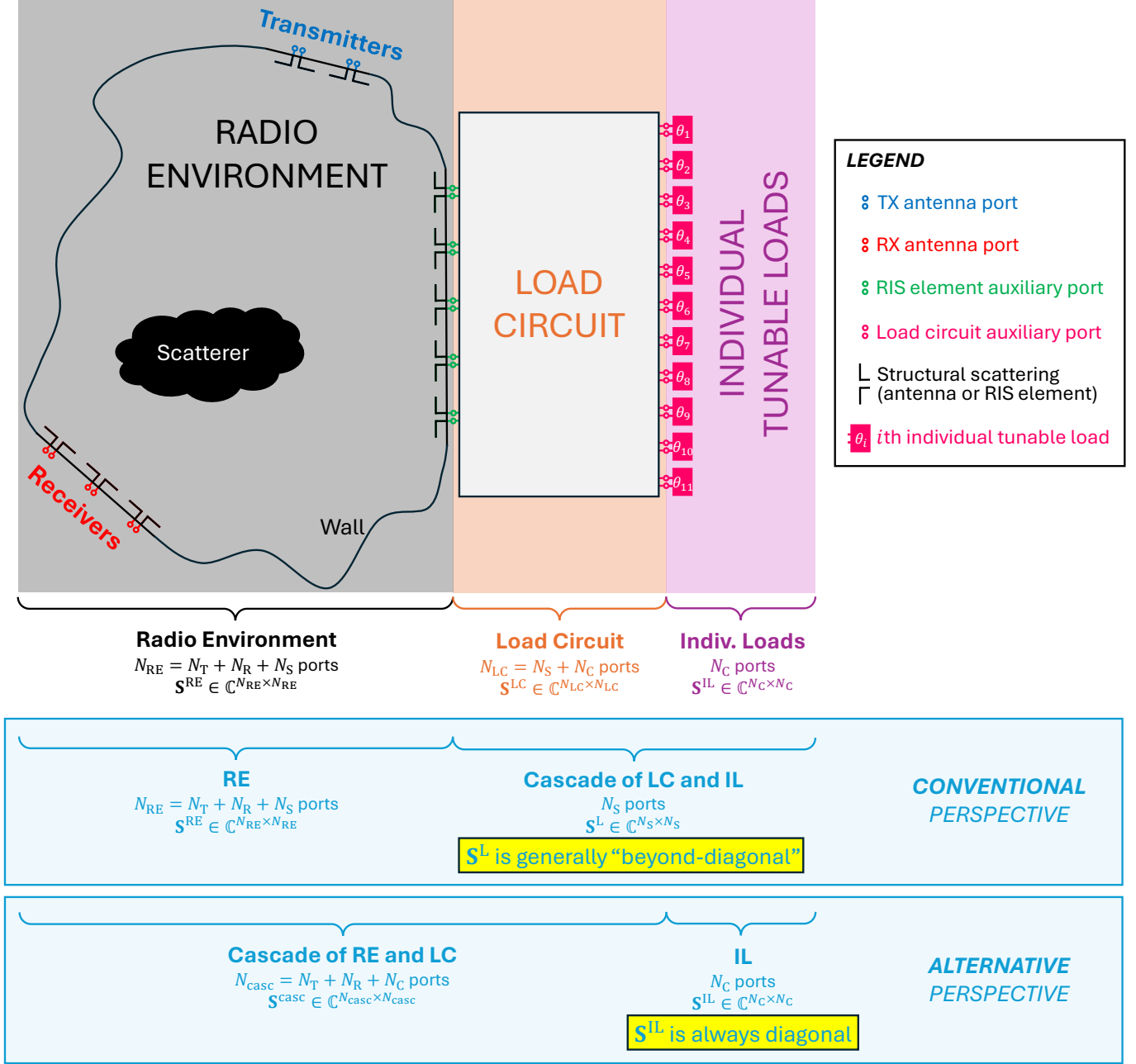


Fig. 1. Generic multi-port chain cascade analysis of BD-RIS-parametrized wireless channels. The radio environment is an N_{RE} -port system characterized by the scattering matrix \mathbf{S}^{RE} , where N_{RE} is the sum of N_T (number of transmitting antennas), N_R (number of receiving antennas) and N_S (number of RIS elements). \mathbf{S}^{RE} lumps together all scattering effects in the radio environment, including scattering originating from objects and walls as well as the structural scattering by the antennas and RIS elements. The N_S auxiliary ports associated with the RIS elements are terminated by a load circuit. The load circuit is itself an N_{LC} -port system characterized by the scattering matrix \mathbf{S}^{LC} , where N_{LC} is the sum of N_S and N_C (number of tunable lumped elements). The N_C ports of the load circuit associated with tunable lumped elements are terminated by individual tunable loads. These constitute an N_C -port system characterized by the diagonal scattering matrix \mathbf{S}^{IL} . (In the case of a conventional D-RIS, each RIS element auxiliary port is directly and uniquely connected to one individual tunable load, implying $N_C = N_S$ and $\mathbf{S}^{LC} = [\mathbf{0}_{N_S} \quad \mathbf{I}_{N_S}; \mathbf{I}_{N_S} \quad \mathbf{0}_{N_S}]$.) The conventional perspective on this chain cascade (albeit never explicit so far) consists in first evaluating the cascade of load circuit and individual tunable loads, which yields a *generally "beyond-diagonal"* scattering matrix \mathbf{S}^L that terminates the RIS element auxiliary ports of the radio environment. The alternative perspective emphasized in this paper is to first evaluate the cascade of radio environment and load circuit; the auxiliary ports of this cascade associated with tunable lumped elements are then terminated by \mathbf{S}^{IL} which is *always diagonal*.

the scattering matrix $\mathbf{S}^L \in \mathbb{C}^{N_S \times N_S}$ which terminates the RIS element auxiliary ports of the radio environment. Let $\mathbf{S}^{IL} \in \mathbb{C}^{N_C \times N_C}$ be a diagonal matrix containing the N_C reflection coefficients of the individual tunable loads. We denote by $\bar{\mathcal{S}}$

and \mathcal{C} the sets of port indices of the load circuit associated with RIS elements and tunable individual loads, respectively.

Then,

$$\mathbf{S}^L = \mathbf{S}_{\mathcal{S}\mathcal{S}}^{\text{LC}} + \mathbf{S}_{\mathcal{S}\mathcal{C}}^{\text{LC}} \left((\mathbf{S}^{\text{IL}})^{-1} - \mathbf{S}_{\mathcal{C}\mathcal{C}}^{\text{LC}} \right)^{-1} \mathbf{S}_{\mathcal{C}\mathcal{S}}^{\text{LC}}, \quad (1)$$

which is generally a ‘‘beyond diagonal’’ matrix except for the D-RIS case with $\mathbf{S}^{\text{LC}} = [\mathbf{0}_{N_{\mathcal{S}}} \quad \mathbf{I}_{N_{\mathcal{S}}}; \mathbf{I}_{N_{\mathcal{S}}} \quad \mathbf{0}_{N_{\mathcal{S}}}]$ in which we simply find $\mathbf{S}^L = \mathbf{S}^{\text{IL}}$, as expected. The fact that \mathbf{S}^L is generally ‘‘beyond diagonal’’ is in line with the conventional understanding of BD-RIS but its origin as defined in Eq. (1) has not been previously pointed out, to the best of our knowledge.

Given \mathbf{S}^L , we can then determine the scattering matrix $\tilde{\mathbf{S}} \in \mathbb{C}^{N_{\mathcal{A}} \times N_{\mathcal{A}}}$, where $N_{\mathcal{A}} = N_{\mathcal{T}} + N_{\mathcal{R}}$, that is ‘‘measurable’’ via the antennas in the radio environment:

$$\tilde{\mathbf{S}} = \mathbf{S}_{\mathcal{A}\mathcal{A}}^{\text{RE}} + \mathbf{S}_{\mathcal{A}\mathcal{S}}^{\text{RE}} \left((\mathbf{S}^L)^{-1} - \mathbf{S}_{\mathcal{S}\mathcal{S}}^{\text{RE}} \right)^{-1} \mathbf{S}_{\mathcal{S}\mathcal{A}}^{\text{RE}}, \quad (2)$$

where \mathcal{A} and \mathcal{S} denote the sets of port indices of the radio environment associated with the antennas and RIS elements, respectively. The wireless channel matrix \mathbf{H} is then simply an off-diagonal block of $\tilde{\mathbf{S}}$:

$$\mathbf{H} = \left[\tilde{\mathbf{S}} \right]_{\mathcal{R}\mathcal{T}}, \quad (3)$$

where \mathcal{R} and \mathcal{T} denote the sets containing the port indices associated with receiving and transmitting antennas, respectively. For completeness, we note that $\mathcal{A} = \mathcal{T} \cup \mathcal{R}$.

Following the procedure detailed for D-RIS based on PhysFad in Ref. [17], we can rewrite the matrix inversion in Eq. (2) as infinite sum of matrix powers:

$$\begin{aligned} \tilde{\mathbf{S}} &= \mathbf{S}_{\mathcal{A}\mathcal{A}}^{\text{RE}} + \mathbf{S}_{\mathcal{A}\mathcal{S}}^{\text{RE}} \left((\mathbf{S}^L)^{-1} - \mathbf{S}_{\mathcal{S}\mathcal{S}}^{\text{RE}} \right)^{-1} \mathbf{S}_{\mathcal{S}\mathcal{A}}^{\text{RE}} \\ &= \mathbf{S}_{\mathcal{A}\mathcal{A}}^{\text{RE}} + \mathbf{S}_{\mathcal{A}\mathcal{S}}^{\text{RE}} \left(\mathbf{I}_{N_{\mathcal{S}}} - \mathbf{S}^L \mathbf{S}_{\mathcal{S}\mathcal{S}}^{\text{RE}} \right)^{-1} \mathbf{S}^L \mathbf{S}_{\mathcal{S}\mathcal{A}}^{\text{RE}} \\ &= \mathbf{S}_{\mathcal{A}\mathcal{A}}^{\text{RE}} + \mathbf{S}_{\mathcal{A}\mathcal{S}}^{\text{RE}} \left(\sum_{k=0}^{\infty} (\mathbf{S}^L \mathbf{S}_{\mathcal{S}\mathcal{S}}^{\text{RE}})^k \right) \mathbf{S}^L \mathbf{S}_{\mathcal{S}\mathcal{A}}^{\text{RE}}, \end{aligned} \quad (4)$$

where the convergence of the infinite series is guaranteed by the fact that we work with passive systems. Specifically, passivity ensures that the spectral radii of \mathbf{S}^L and $\mathbf{S}_{\mathcal{S}\mathcal{S}}^{\text{RE}}$ do not exceed unity, and hence, due to submultiplicativity, the spectral radius of $\mathbf{S}^L \mathbf{S}_{\mathcal{S}\mathcal{S}}^{\text{RE}}$ cannot exceed unity. Upon truncation of the infinite series in the last line of Eq. (4) after its first term, i.e., $k = 0$, we obtain

$$\tilde{\mathbf{S}} \approx \mathbf{S}_{\mathcal{A}\mathcal{A}}^{\text{RE}} + \mathbf{S}_{\mathcal{A}\mathcal{S}}^{\text{RE}} \mathbf{S}^L \mathbf{S}_{\mathcal{S}\mathcal{A}}^{\text{RE}}. \quad (5)$$

Upon inserting Eq. (5) into Eq. (3), we get

$$\mathbf{H} \approx \mathbf{S}_{\mathcal{R}\mathcal{T}}^{\text{RE}} + \mathbf{S}_{\mathcal{R}\mathcal{S}}^{\text{RE}} \mathbf{S}^L \mathbf{S}_{\mathcal{S}\mathcal{T}}^{\text{RE}}, \quad (6)$$

which is the widespread simplified cascaded model of RIS-parametrized channels, decomposing the end-to-end channel into a contribution that did not encounter the RIS (the first term), and a contribution that interacted once with the RIS (the second term); \mathbf{S}^L is diagonal for D-RIS and ‘‘beyond-diagonal’’ for BD-RIS. Note that the truncation at $k = 0$ is potentially a very strong assumption and Eq. (6) is generally *not* physics-compliant.

C. Alternative perspective

Alternatively, we can begin by evaluating the cascade of RE and LC, whose auxiliary ports associated with the tunable lumped elements will then be terminated by IL. The cascade of RE and LC is characterized by

$$\mathbf{S}^{\text{casc}} = \begin{bmatrix} \mathbf{S}_{\mathcal{A}\mathcal{A}}^{\text{casc}} & \mathbf{S}_{\mathcal{A}\mathcal{C}}^{\text{casc}} \\ \mathbf{S}_{\mathcal{C}\mathcal{A}}^{\text{casc}} & \mathbf{S}_{\mathcal{C}\mathcal{C}}^{\text{casc}} \end{bmatrix} \in \mathbb{C}^{N_{\text{casc}} \times N_{\text{casc}}}, \quad (7)$$

where $N_{\text{casc}} = N_{\mathcal{A}} + N_{\mathcal{C}}$, and \mathcal{A} and \mathcal{C} denote the sets of port indices associated with antennas and tunable lumped elements, respectively. The analytical expression for \mathbf{S}^{casc} is obtained via the well-established ‘‘Redheffer star product’’ [41]–[44]:

$$\begin{aligned} \mathbf{S}_{\mathcal{A}\mathcal{A}}^{\text{casc}} &= \mathbf{S}_{\mathcal{A}\mathcal{A}}^{\text{RE}} - \mathbf{S}_{\mathcal{A}\mathcal{S}}^{\text{RE}} \mathbf{S}_{\mathcal{S}\mathcal{S}}^{\text{LC}} \mathbf{X}_1 \mathbf{S}_{\mathcal{S}\mathcal{A}}^{\text{RE}}, \\ \mathbf{S}_{\mathcal{A}\mathcal{C}}^{\text{casc}} &= -\mathbf{S}_{\mathcal{A}\mathcal{S}}^{\text{RE}} \mathbf{X}_2 \mathbf{S}_{\mathcal{S}\mathcal{C}}^{\text{LC}}, \\ \mathbf{S}_{\mathcal{C}\mathcal{A}}^{\text{casc}} &= -\mathbf{S}_{\mathcal{C}\mathcal{S}}^{\text{LC}} \mathbf{X}_1 \mathbf{S}_{\mathcal{S}\mathcal{A}}^{\text{RE}}, \\ \mathbf{S}_{\mathcal{C}\mathcal{C}}^{\text{casc}} &= \mathbf{S}_{\mathcal{C}\mathcal{C}}^{\text{LC}} - \mathbf{S}_{\mathcal{C}\mathcal{S}}^{\text{LC}} \mathbf{S}_{\mathcal{S}\mathcal{S}}^{\text{RE}} \mathbf{X}_2 \mathbf{S}_{\mathcal{S}\mathcal{C}}^{\text{LC}}, \end{aligned} \quad (8)$$

where

$$\begin{aligned} \mathbf{X}_1 &= (\mathbf{S}_{\mathcal{S}\mathcal{S}}^{\text{RE}} \mathbf{S}_{\mathcal{S}\mathcal{S}}^{\text{LC}} - \mathbf{I}_{N_{\mathcal{S}}})^{-1}, \\ \mathbf{X}_2 &= (\mathbf{S}_{\mathcal{S}\mathcal{S}}^{\text{LC}} \mathbf{S}_{\mathcal{S}\mathcal{S}}^{\text{RE}} - \mathbf{I}_{N_{\mathcal{S}}})^{-1}. \end{aligned} \quad (9)$$

This expression for the cascade of RE and LC is mathematically more complex than that for the cascade of LC and IL provided in the previous section because both RE and LC have ‘‘free’’ (unconnected) ports after the connection of RE and LC whereas only LC but not IL has free ports after the connection of LC and IL [44].

Given \mathbf{S}^{casc} , we can then determine $\tilde{\mathbf{S}}$ as follows:

$$\tilde{\mathbf{S}} = \mathbf{S}_{\mathcal{A}\mathcal{A}}^{\text{casc}} + \mathbf{S}_{\mathcal{A}\mathcal{C}}^{\text{casc}} \left((\mathbf{S}^{\text{IL}})^{-1} - \mathbf{S}_{\mathcal{C}\mathcal{C}}^{\text{casc}} \right)^{-1} \mathbf{S}_{\mathcal{C}\mathcal{A}}^{\text{casc}}. \quad (10)$$

The wireless channel matrix is then again obtained via Eq. (3). The development outlined in this subsection hence constitutes the physics-compliant *diagonal* representation for wireless channels parametrized by BD-RIS because \mathbf{S}^{IL} in Eq. (10) is always diagonal.

D. Comparison

Obviously, the expression for $\tilde{\mathbf{S}}$ from Eq. (10) must be equal to the expression for $\tilde{\mathbf{S}}$ from Eq. (2) since we did not make any assumptions to obtain either of these equations. It is instructive to compare the role of corresponding quantities in Eq. (2) and Eq. (10):

$$\mathbf{S}^{\text{RE}} \leftrightarrow \mathbf{S}^{\text{casc}}, \quad (11a)$$

$$\mathbf{S}^L \leftrightarrow \mathbf{S}^{\text{IL}}, \quad (11b)$$

$$\mathcal{S} \leftrightarrow \mathcal{C}. \quad (11c)$$

In the conventional perspective, the primary ports are those comprised in $\mathcal{A} \cup \mathcal{S}$, and the ports of RE from \mathcal{S} are terminated by \mathbf{S}^L which is *generally* ‘‘beyond-diagonal’’. In the alternative perspective, the primary ports are those comprised in $\mathcal{A} \cup \mathcal{C}$, and the ports of the cascade of RE and LC from \mathcal{C} are terminated by \mathbf{S}^{IL} which is *always diagonal*.

III. DETERMINING \mathbf{S}^{LC}

At the core of our theoretical developments in the previous section is \mathbf{S}^{LC} , the scattering matrix characterizing the static load circuit which connects the RIS elements to the tunable individual loads. The existence of \mathbf{S}^{LC} has to date not been brought up explicitly in the BD-RIS literature, to the best of our knowledge, such that we dedicate this section to discussing how to determine the values of \mathbf{S}^{LC} analytically for canonical examples of ideal load circuits, as well as how it could be determined in numerical full-wave simulations and to what extent it could be determined experimentally. At the end of this section, we go on to argue that, in fact, operationally there is no need to explicitly know \mathbf{S}^{LC} and that what we need to know or estimate is \mathbf{S}^{casc} but not its breakdown into \mathbf{S}^{RE} and \mathbf{S}^{LC} .

A. Theoretical canonical examples

Theoretically studied tunable circuits that terminate RIS elements in BD-RIS typically include tunable lumped elements that are connected without loss, delay and dispersion to each other and/or the RIS element auxiliary ports and/or ground. Under these simplifying assumptions, the multi-port network description of the circuit can be determined analytically.

Thus far, existing theoretical studies of BD-RIS directly obtained \mathbf{S}^{L} without explicitly identifying \mathbf{S}^{LC} and \mathbf{S}^{IL} . More specifically, as detailed in Eq. (13) of Ref. [7] (based on Eq. (6) of Ref. [45]), the admittance representation \mathbf{Y}^{L} of the circuit is obtained in closed form, which can then be transformed to \mathbf{S}^{L} , if desired.

We begin by analytically considering a simple ideal two-port T network containing three lumped impedances Z_1 , Z_2 and Z_3 , as sketched in Fig. 1A. The characteristic impedance of the two transmission lines attached to the two ports is $Z_0 = 50 \Omega$. Recall that black lines denote connections without loss, delay or dispersion.

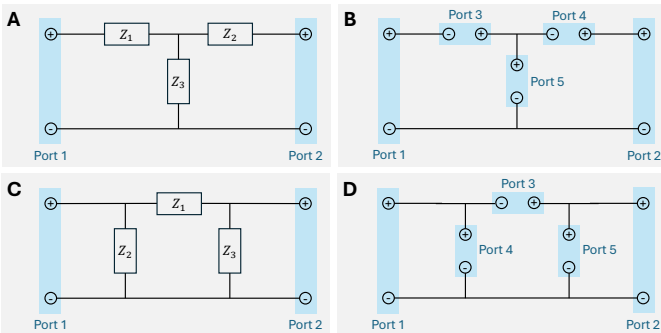


Fig. 2. (A) Ideal 2-port T network. (B) The three impedances in (A) are replaced by auxiliary ports, yielding a 5-port network whose scattering matrix can be determined analytically, see the Appendix and Eq. (12). (C) Ideal 2-port π network. (D) The three impedances in (C) are replaced by auxiliary ports, yielding a 5-port network whose scattering matrix can be determined analytically, see Eq. (13).

Using basic circuit analysis, as detailed in the Appendix, we readily obtain the 5×5 scattering matrix of the circuit from

Fig. 2B:

$$\mathbf{S}^{\text{LC},\text{T}} = \begin{bmatrix} 0.25 & 0.25 & -0.75 & -0.25 & 0.5 \\ 0.25 & 0.25 & 0.25 & 0.75 & 0.5 \\ -0.75 & 0.25 & 0.25 & -0.25 & 0.5 \\ -0.25 & 0.75 & -0.25 & 0.25 & -0.5 \\ 0.5 & 0.5 & 0.5 & -0.5 & 0 \end{bmatrix}. \quad (12)$$

We have verified this result with three sanity checks, as detailed in the Appendix.

A similar analysis for a π network whose three lumped impedances have been replaced by auxiliary ports yields

$$\mathbf{S}^{\text{LC},\pi} = \begin{bmatrix} -0.25 & 0.25 & -0.5 & 0.75 & 0.25 \\ 0.25 & -0.25 & 0.5 & 0.25 & 0.75 \\ -0.5 & 0.5 & 0 & -0.5 & 0.5 \\ 0.75 & 0.25 & -0.5 & -0.25 & 0.25 \\ 0.25 & 0.75 & 0.5 & 0.25 & -0.25 \end{bmatrix}. \quad (13)$$

Again, we verified this result with three sanity checks. A reconfigurable ideal π network like the one we study was considered in Fig. 3(a) of Ref. [7] for a group-connected BD-RIS with a group size of two.

The same exercise can be repeated for more complex ideal reconfigurable impedance networks such as the one from Fig. 2(b) in Ref. [7] but manual execution of the required circuit analysis rapidly becomes tiresome; already for the example from Fig. 2(b) in Ref. [7] the dimensions of the sought-after \mathbf{S}^{LC} would be 14×14 . Therefore, for studies of large and/or realistic (as opposed to ideal) reconfigurable impedance networks, the numerical or experimental approaches described in the next two subsections are more suitable.

B. Numerical full-wave simulations

Whereas the previous subsection covered theoretical ideal load circuits that can be analyzed analytically, we now turn our attention to load circuits that can be realized in practise. These can generally not avoid the effects of loss, delay and dispersion, and in most cases, an analytical expression for \mathbf{S}^{LC} will not exist. Nonetheless, it is reasonable to assume that for practical studies of realistic BD-RIS designs a detailed layout of the circuit terminating the RIS elements is available. Indeed, such a layout will be an inevitable pre-requisite for any experimentally realized prototype fabrication. Consequently, this circuit can be simulated numerically in full-wave solvers. In fact, a single full-wave simulation is sufficient to obtain \mathbf{S}^{LC} if one simply places lumped ports at the locations of the tunable lumped elements. Incidentally, this is exactly the procedure that was already implemented in Ref. [28] to extract the analytically intractable scattering matrix of a highly complex on-chip radio environment parametrized by a D-RIS. As mentioned earlier, a radio environment parametrized by a D-RIS is conceptually exactly the same problem as a load circuit parametrized by tunable individual loads. To summarize, for any arbitrarily complex load circuit design, a single full-wave simulation can yield \mathbf{S}^{LC} .

C. Experimental estimation

In this subsection, we discuss the extent to which \mathbf{S}^{LC} could be estimated experimentally. A pivotal requirement for such an experimental estimation would be the possibility to input and output waves through the load circuit ports connected to the RIS elements (i.e., ports whose indices are in the set $\bar{\mathcal{S}}$); this could be possible, for instance, before connecting the RIS and the load circuit. The considered problem is analogous to the problem of physics-compliant end-to-end channel estimation with a D-RIS that was tackled in Refs. [19], [30]. Indeed, the load circuit is a multi-port network characterized by \mathbf{S}^{LC} that is terminated by individual tunable loads. Based on experimental measurements at the ports of the load circuit from set $\bar{\mathcal{S}}$ for different terminations of the ports from set \mathcal{C} , it is provably impossible to unambiguously determine \mathbf{S}^{LC} experimentally because at least sign ambiguities on off-diagonal terms associated with the ports from set \mathcal{C} will remain [16], [30]. If not at least three distinct and characterized individual load states are available at the ports from \mathcal{C} , additional ambiguities about \mathbf{S}^{LC} ensue. However, operationally, these ambiguities are not problematic because as long as \mathbf{S}^{L} is correctly predicted we have everything we need to terminate the ports of \mathbf{S}^{RE} from set \mathcal{S} and thus determine $\tilde{\mathbf{S}}$ and \mathbf{H} . Indeed, Ref. [19] accurately predicted wireless end-to-end channels in an unknown complex medium as a function of the binary configuration of a D-RIS prototype with unknown characteristics. The infinite set of possible parameter values should even facilitate the estimation of a plausible \mathbf{S}^{LC} (and \mathbf{S}^{IL} if it is unknown) that yields an accurate prediction for \mathbf{S}^{L} .

D. Do we need to know \mathbf{S}^{LC} explicitly?

This section was dedicated to discussing various routes to determining \mathbf{S}^{LC} , a quantity that is at the core of the physics-compliant diagonal representation of BD-RIS parametrized channels put forth in the present paper. Although this section is pedagogically important to substantiate the theory developed in the previous section, arguably, *in practise it is not even necessary to explicitly know \mathbf{S}^{LC}* .

Indeed, in practise, the most compact modeling approach would directly map the configuration of the individual tunable loads to the end-to-end wireless channels. The primary entities are the antennas and the tunable lumped elements. Meanwhile, the RIS elements are merely a detail of how these primary entities are coupled to each other. As long as we know \mathbf{S}^{casc} , operationally there is no need to break it down into \mathbf{S}^{RE} and \mathbf{S}^{LC} . Therefore, in the next section, we propose a scheme for end-to-end channel estimation and optimization that only estimates \mathbf{S}^{casc} in order to successfully predict \mathbf{H} as a function of the tunable individual loads.

IV. DIRECTLY APPLYING D-RIS CHANNEL ESTIMATION AND OPTIMIZATION ALGORITHMS TO BD-RIS

This section is dedicated to demonstrating the feasibility of directly applying channel estimation and optimization algorithms originally developed for D-RIS to BD-RIS-parametrized channels, based on an experimentally grounded case study. We first describe the considered scenario, then channel estimation, and finally channel optimization.

A. Considered scenario grounded in an experiment

To ground the considered scenario in an experimental reality involving unknown rich scattering, we have placed eight commercial antennas (AEACBK081014-S698, designed for operation between 698 MHz and 2.69 GHz for GSM, SPRS and 4G (LTE)) inside a reverberation chamber (1.75 m \times 1.50 m \times 2.00 m) and measured the corresponding 8×8 scattering matrix with an eight-port vector network analyzer (Keysight M9005A) at $f = 800$ MHz. The obtained scattering matrix is used as \mathbf{S}^{RE} in this case study. We consider a SISO link involving one transmitting and one receiving antenna, and the remaining six antennas are the RIS elements. The annotations on the photographic image in Fig. 3 highlight this setup. As sketched in the right part of Fig. 3, the six RIS elements are split into three groups of size two that are considered to be connected to ideal π networks, each of which is parametrized by three impedances. We assume that each impedance represents a PIN diode with two possible states whose characteristics are chosen according to those documented for a commercially available PIN diode (MADP-000907-14020x [46]). Specifically, the two possible load impedances are $\eta^{\text{ON}} = 5.2 \Omega$ and $\eta^{\text{OFF}} = (j\omega C)^{-1} = -7.96j \times 10^3 \Omega$, where $j = \sqrt{-1}$, $\omega = 2\pi f$ and $C = 25$ fF. The corresponding reflection coefficients are $r_1 = (\eta^{\text{ON}} - Z_0)/(\eta^{\text{ON}} + Z_0) = -0.81$ and $r_2 = (\eta^{\text{OFF}} - Z_0)/(\eta^{\text{OFF}} + Z_0) = 1.00 - 0.01j$. To recapitulate key parameters: $N_{\text{T}} = 1$, $N_{\text{R}} = 1$, $N_{\text{A}} = N_{\text{T}} + N_{\text{R}} = 2$, $N_{\text{S}} = 6$ and $N_{\text{C}} = 9$.

Our experimental measurements hence fix the entries of \mathbf{S}^{RE} , Eq. (13) fixes the entries of the three diagonal blocks of the block-diagonal matrix \mathbf{S}^{LC} , and the two possible values that the diagonal entries of the diagonal matrix \mathbf{S}^{IL} can take are r_1 and r_2 derived from the PIN diode's data sheet. We can consequently evaluate \mathbf{S}^{L} using Eq. (1) or via the known admittance matrix of an ideal π network. We can also evaluate

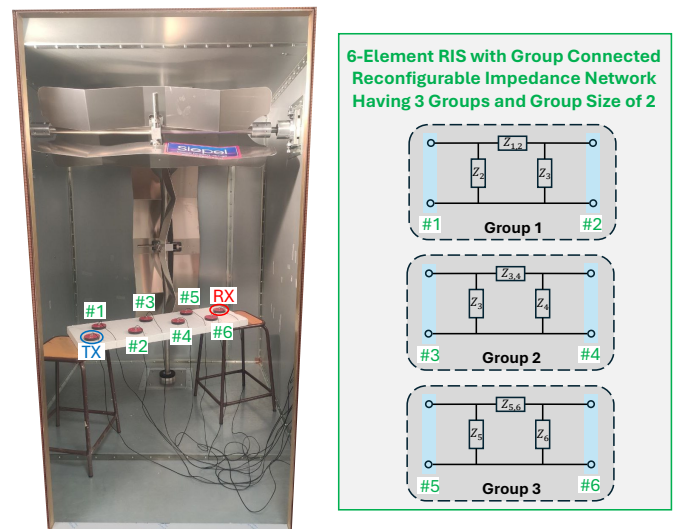


Fig. 3. Experimentally grounded study of a SISO link inside a rich-scattering environment parametrized by a 6-element RIS with group-connected reconfigurable impedance network having three groups and group size two.

\mathbf{S}^{casc} using Eq. (8). Finally, we can determine $\tilde{\mathbf{S}}$ (and thus \mathbf{H}) using Eq. (2) based on \mathbf{S}^{RE} and \mathbf{S}^{L} or using Eq. (10) based on \mathbf{S}^{casc} and \mathbf{S}^{IL} . For the considered SISO problem, \mathbf{H} is a scalar (the off-diagonal entry of $\tilde{\mathbf{S}}$) such that we denote it by h in the following. For a given binary configuration $\mathbf{b} \in \mathbb{C}^{N_C \times 1}$ of the nine tunable load impedances, we can hence identify the corresponding \mathbf{S}^{IL} and ultimately the corresponding h . We verified that both the conventional and the alternative route to evaluating h yields exactly the same value for multiple random choices of \mathbf{b} . Altogether, to the best of our knowledge, this constitutes the first study of a BD-RIS-parametrized wireless channel for which the utilized parameters are grounded in an experimental reality.

To perform physics-compliant end-to-end channel estimation and optimization, we simulate a scenario in which we can configure the reconfigurable impedance network to any desired binary configuration \mathbf{b} and measure the corresponding wireless channel $h(\mathbf{b})$. Of course, we obtain $h(\mathbf{b})$ as detailed in the previous paragraph, but once the pairs $\{\mathbf{b}, h(\mathbf{b})\}$ are generated, we assume that we only know the pairs $\{\mathbf{b}, h(\mathbf{b})\}$ and do not have any knowledge of r_1 , r_2 , \mathbf{S}^{LC} or \mathbf{S}^{RE} . We thereby simulate a true end-to-end channel estimation and optimization problem without any a priori knowledge of the characteristics of the radio environment, the load circuit or the tunable lumped elements.

B. Channel estimation

The literature contains a few theoretical studies on channel estimation in scenarios involving BD-RIS [47], [48]. However, these are based on simplified cascaded channel models. Here, we tackle the problem of physics-compliant end-to-end channel estimation of BD-RIS parametrized channels in a scenario that is grounded in experimental data. We highlight that thanks to the diagonal representation of the BD-RIS-parametrized channel we only need to estimate some version of \mathbf{S}^{casc} and \mathbf{S}^{IL} but not the breakdown of \mathbf{S}^{casc} into \mathbf{S}^{RE} and \mathbf{S}^{LC} . (The words ‘‘some version’’ in the previous sentence hint at the fact that ambiguities are inevitable and not problematic, as discussed below.)

1) *Problem statement:* Our ultimate goal in end-to-end channel estimation is to be able to map any conceivable \mathbf{b} to the corresponding end-to-end wireless channel $h(\mathbf{b})$:

$$\mathbf{b} \rightarrow h(\mathbf{b}). \quad (14)$$

As stated earlier, we do not assume to know anything but pairs of $\{\mathbf{b}, h(\mathbf{b})\}$.

We hence face a parameter estimation problem. The most compact approach is based on the diagonal representation of the BD-RIS-parametrized channel. It consists in determining a set of parameters comprising the entries of \mathbf{S}^{casc} as well as the two possible values r_1 and r_2 that each diagonal entry of \mathbf{S}^{IL} can take such that we correctly predict h using Eq. (10) and Eq. (3) for any given \mathbf{b} .

Fortunately, this problem directly maps into the problem of physics-compliant end-to-end channel estimation for D-RIS for which experimentally validated solutions were already presented in Refs. [12], [30]. Key insights from Refs. [12], [30]

as transposed to our BD-RIS-based scenario are summarized as follows:

- 1) The number of parameters to be estimated is

$$\begin{aligned} N_{\text{params}} &= 2 \left(2 + \frac{(N_A + N_C)(N_A + N_C + 1)}{2} \right) \\ &= 4 + (N_A + N_C)(N_A + N_C + 1) \\ &= 136, \end{aligned} \quad (15)$$

where the first term inside the brackets corresponds to the two possible reflection coefficients r_1 and r_2 of the individually tunable lumped elements, the second term inside the brackets corresponds to the entries of \mathbf{S}^{casc} which is symmetric due to reciprocity, and the factor two in front of the brackets takes into account that the variables are complex-valued. Note that the number of parameters to be estimated neither depends on N_S nor on the complexity of the radio environment nor on the complexity of the load circuit.

- 2) Any set of parameters that correctly predicts $h(\mathbf{b})$ is satisfactory. There are inevitable ambiguities in the parameter values because the parameter estimation problem is not sufficiently constrained to yield a unique solution. However, these ambiguities do not pose any problem with respect to our goal of accurately predicting $h(\mathbf{b})$.
- 3) The parameter estimation problem can be solved in closed form [30] or via gradient descent [19], [30]. In the case of a gradient-descent approach, the parameters can be estimated purely based on non-coherent measurements [19], [30]. Further benefits of the gradient-descent approach include its compatibility with opportunistic configuration switching and a better robustness against noise. The latter originates from the fact that the changes of h between any two measurements are larger because on average half the tunable lumped elements have changed their state, as well as from the fact that any arbitrary number of measurements can readily be taken into account.

Here, we follow the gradient-descent approach put forth for the D-RIS scenario in Ref. [19].

2) *Algorithm:* Our physics-compliant end-to-end channel estimation algorithm closely follows that proposed in Sec. IV of Ref. [30]. However, our present problem differs from that considered in Ref. [30] in that we only measure h instead of $\tilde{\mathbf{S}}$ and in that we do not know the values of r_1 and r_2 . Hence, we seek to estimate the entries of \mathbf{S}^{casc} (except for the diagonal ones in the block $\mathcal{A}\mathcal{A}$) as well as r_1 and $r_2 - r_1$ simultaneously. The earlier gradient-descent proposal from Ref. [19] did not use an advantageous two-step procedure but it did also treat a problem with unknown load characteristics. Our algorithmic implementation consists simply in optimizing the sought-after parameters via gradient descent such that a cost function quantifying the difference between the predicted and ground truth values of the difference of h between successive configurations of the individual tunable loads is minimized. Additional implementation details can be found in Ref. [30].

3) *Results:* Based on the same data set, we ran our end-to-end channel estimation algorithm twice. Two examples of estimated parameter sets are plotted in Fig. 4A and compared to the known ground truth values. Except for the \mathcal{RT} block of \mathbf{S}^{casc} (which is a scalar in our case study), clear differences to the ground truth as well as between the two estimates are apparent, as expected due to the inevitable ambiguities. Nonetheless, the estimated set of parameters allows us to accurately predict $h(\mathbf{b})$ for arbitrary unseen \mathbf{b} , as evidenced by the comparison between predicted and ground-truth values of $h(\mathbf{b})$ for arbitrary unseen \mathbf{b} in Fig. 4B. The inevitable ambiguities are thus not problematic for our goal of identifying an accurate mapping $\mathbf{b} \rightarrow h(\mathbf{b})$. We have hence successfully determined a “purely physics-based digital twin” for our BD-RIS parametrized channel without having explicitly identified \mathbf{S}^{RE} or \mathbf{S}^{LC} . In fact, our method does not even require knowledge of N_S .

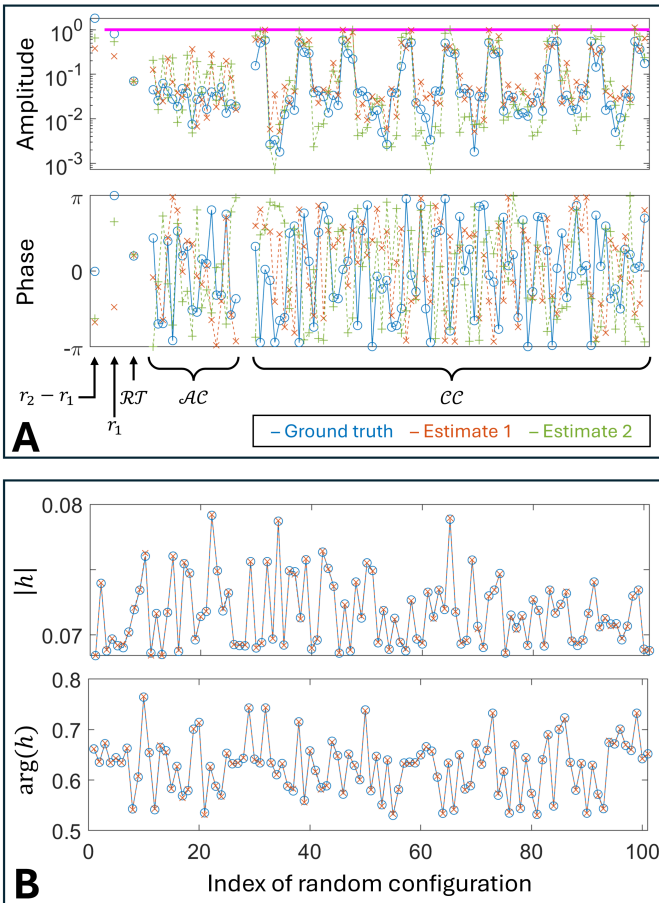


Fig. 4. (A) Amplitude and phase of the experimentally grounded ground truth (blue) and two separate estimates (red and green) of the parameters within the diagonal representation of the BD-RIS-parametrized channel: $r_2 - r_1$, r_1 , the \mathcal{RT} block of \mathbf{S}^{casc} (which is just a scalar here), the \mathcal{AC} block of \mathbf{S}^{casc} (which is vectorized for ease of display here), and the \mathcal{CC} block of \mathbf{S}^{casc} (which is vectorized for ease of display here). (B) Amplitude and phase of ground truth (blue) and predicted (red) end-to-end wireless channel h for 100 random unseen configurations of the reconfigurable load network.

C. RSSI Optimization

Based on the estimated end-to-end channel model from the previous subsection, we can identify a configuration of the considered reconfigurable impedance network that maximizes the received signal strength indicator (RSSI, here defined as $|h|^2$) on the considered SISO link. Due to the non-linear dependence of h on \mathbf{b} (see also Ref. [17]) and the binary constraint on the possible entries of \mathbf{b} , we use the simple coordinate ascent approach summarized in Algorithm 1 to identify an optimized configuration \mathbf{b}_{opt} . This requires many forward evaluations, i.e., mappings from \mathbf{b} to $h(\mathbf{b})$. However, we do not have to perform the full matrix inversion seen in Eq. (10) for every forward evaluation. Instead, we can use the Woodbury identity to efficiently update previous matrix inverses, as discussed in detail for the case of a D-RIS in the PhysFad formalism in Ref. [20]. Again, we hence benefit from the diagonal representation of the BD-RIS-parametrized channel to recycle previous algorithmic developments in the realm of D-RIS.

Algorithm 1: RSSI optimization via coordinate ascent.

- 1 Choose a random binary vector $\mathbf{b}_{\text{curr}} \in \mathbb{C}^{N_C \times 1}$.
 - 2 Evaluate the corresponding RSSI $R_{\text{curr}} = |h(\mathbf{b}_{\text{curr}})|^2$.
 - 3 $k \leftarrow 0$.
 - 4 **while** $k < 10N_C$ **do**
 - 5 Define i as a randomly chosen integer such that $1 \leq i \leq N_C$.
 - 6 $\mathbf{b}' \leftarrow \mathbf{b}_{\text{curr}}$ with the i th entry flipped.
 - 7 Evaluate the corresponding RSSI $R' = |h(\mathbf{b}')|^2$.
 - 8 **if** $R' > R_{\text{curr}}$ **then**
 - 9 $R_{\text{curr}} \leftarrow R'$.
 - 10 $\mathbf{b}_{\text{curr}} \leftarrow \mathbf{b}'$.
 - 11 **end**
 - 12 $k \leftarrow k + 1$.
 - 13 **end**
 - 14 Repeat steps 1 to 13 ten times, define the globally best R_{curr} as R_{opt} , and the corresponding \mathbf{b}_{curr} as \mathbf{b}_{opt} .
- Output:** Optimized configuration \mathbf{b}_{opt} and corresponding R_{opt} .
-

A comparison of the expected maximal RSSI with the optimized RIS configuration \mathbf{b}_{opt} benchmarked against the ground-truth RSSI for that configuration is shown in Fig. 5. No difference is apparent upon visual inspection. For reference, the probability density function of the RSSI obtained by evaluating the RSSI for a series of random configurations is also shown. Furthermore, since an exhaustive search of the 2^9 possible configuration is feasible for the considered small-scale case study, we also identified the globally optimal configuration (using the ground-truth simulations without reliance on the estimated channel model) which coincides with the one obtained via Algorithm 1.

The RSSI enhancement enabled by the considered BD-RIS is moderate in the considered example due to the small scale of the RIS which comprises only six elements. However, this example is sufficient to demonstrate the key point of our paper, namely that we can successfully optimize our

BD-RIS based on the end-to-end channel estimate from the previous section. Both channel estimation and optimization pivotally rely on the diagonal representation of the BD-RIS-parametrized channel.

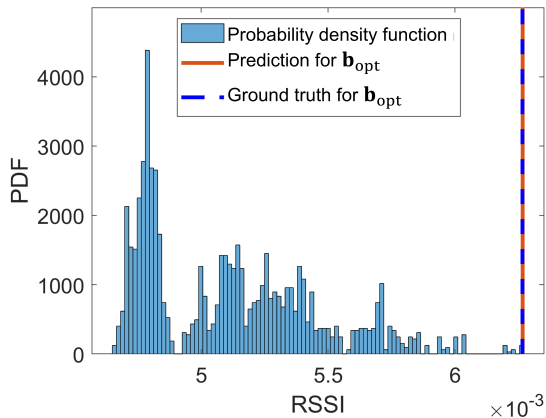


Fig. 5. Probability density function of the RSSI for the considered SISO link, as well as predicted and ground-truth RSSI for the configuration \mathbf{b}_{opt} obtained with Algorithm 1 based on the end-to-end channel estimate from Sec. IV.

V. RELATION TO PHYSFAD

Thus far, we have only discussed circuit-theory-based physics-compliant modeling of BD-RIS parametrized channels. For the D-RIS case, an alternative (but ultimately equivalent) physics-compliant approach based on a coupled-dipole formalism exists. It was introduced as PhysFad [18] and constituted the basis of the first experimental validation of a physics-compliant channel model for arbitrarily complex D-RIS-parametrized rich-scattering channels as well as various frugal physics-compliant end-to-end channel estimation protocols [12]. The basic approach of the coupled-dipole formalism consists in assigning a dipole to each primary wireless entity (antennas and tunable lumped elements). The dipoles are characterized by their polarizability which is tunable in the case of the tunable lumped elements. The dipoles are coupled to each other via background Green's functions. An interaction matrix is set up, composed of the sum of a diagonal matrix containing the inverse polarizabilities and a symmetric matrix containing the background Green's functions. The top left block of the inverse of this interaction matrix yields $\hat{\mathbf{S}}$. Whereas circuit theory treats systems as black boxes, the coupled-dipole approach describes the physical wave-matter interactions inside the systems, enabling insights that are not accessible via circuit theory such as the method for performing conjugate beamforming without pilot exchange purely based on user motion that was proposed and experimentally demonstrated in Ref. [49].

To date, it remained unclear how exactly the PhysFad formalism could be applied to BD-RIS-parametrized wireless channels. Given the presented physics-compliant diagonal representation of BD-RIS-parametrized channels, the compatibility with the PhysFad framework is now clear: The dipoles are associated with the antennas and tunable lumped elements, and the background Green's functions account for

the potentially highly complex scattering in the cascade of the radio environment and the load circuit.

VI. CONCLUSION

To summarize, we have introduced a new *diagonal* representation of BD-RIS-parametrized channels that is fully physics-compliant. Our key insight relates to the realization that the BD-RIS reconfigurable impedance network, irrespective of its detailed architecture, is itself a multi-port network with a subset of auxiliary ports terminated by individual tunable loads. This implies that a BD-RIS-parametrized channel results from a chain cascade of radio environment (RE), load circuit (LC) and individual tunable loads (IL). Whereas conventionally one considers the auxiliary ports of RE associated with RIS elements to be terminated by a load that is the cascade of LC and IL (and hence characterized by a generally beyond-diagonal matrix), we alternatively consider the cascade of RE and LC whose auxiliary ports associated with tunable load elements are terminated by IL (which is always characterized by a diagonal matrix). A key consequence of this diagonal representation is that we can directly apply D-RIS algorithms for channel estimation and optimization to BD-RIS-parametrized channels. We demonstrated this in the first experimentally grounded case study of BD-RIS with an example of physics-compliant end-to-end channel estimation and RSSI maximization. Importantly, we only sought a representation of the characteristics of the cascade of RE and LC, without ever requiring its breakdown into RE and LC, and without even requiring a removal of ambiguities. Hence, operationally, there is in principle no need to explicitly know \mathbf{S}^{RE} and \mathbf{S}^{LC} ; nonetheless, for pedagogical reasons, we also demonstrated how to obtain \mathbf{S}^{LC} analytically for canonical ideal reconfigurable impedance networks, and we discussed how to obtain it numerically or experimentally for practical realizations. Along the way, we have furthermore rigorously derived the relation between physics-compliant and simplified cascaded models of BD-RIS-parametrized arbitrarily complex (i.e., potentially rich-scattering) channels, as well as how the latter can be represented by coupled-dipole-based physics-compliant models like PhysFad.

APPENDIX

In this Appendix, we illustrate the procedure for analytically determining \mathbf{S}^{LC} for an ideal T network whose impedances have been replaced by auxiliary ports, as sketched in Fig. 2B. The characteristic impedances of the transmission lines attached to the ports are assumed to be $Z_0 = 50 \Omega$. We follow the procedure outlined in Pozar's book [50]: " S_{ij} is found by driving port j with an incident wave of voltage V_j^+ and measuring the reflected wave amplitude V_i^- coming out of port i . The incident waves on all ports except the j th port are set to zero, which means that all ports should be terminated in matched loads to avoid reflections." We also detail various sanity checks to confirm that our results are correct.

A. Step-by-step procedure

- 1) Define the ports, including their numbering and polarity, as done in Fig. 6A.
- 2) Replace all but the i th port with matched loads, and replace the i th port with a matched source, as done in Fig. 6B for $i = 1$. A matched source is a voltage generator in series with a matched load, denoting the generator's voltage with V_g .
- 3) Determine the voltage drop V_j across the j th port, as illustrated using voltmeters in Fig. 6B. This is a basic circuit analysis exercise that can be performed in closed form. Alternatively, circuit analysis tools like <https://falstad.com/circuit/> can be used.
- 4) Evaluate

$$S_{ii}^{\text{LC,T}} = \frac{V_i^-}{V_i^+} = \frac{V_i - V_i^+}{V_i^+} = \frac{V_i - (V_g/2)}{V_g/2}. \quad (16)$$

- 5) Evaluate

$$S_{ji}^{\text{LC,T}} = \frac{V_j^-}{V_i^+} = \frac{V_j}{V_g/2} \quad (17)$$

for each $j \neq i$.

- 6) Repeat for each i .

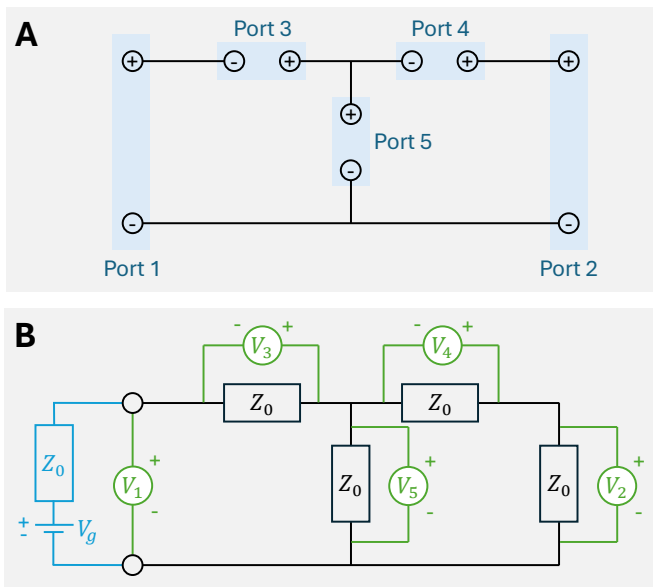


Fig. 6. (A) Ideal T network with auxiliary ports replacing the three impedances. Polarities are defined for each of the five ports. (B) Setup to determine column $i = 1$ of $\mathbf{S}^{\text{LC,T}}$. All ports except for the i th port are terminated with matched loads (Z_0). A matched source (voltage generator in series with a matched load, drawn in light blue) is connected to the i th port. The voltage drops across all ports are monitored with the voltmeters drawn in green.

B. Sanity checks

For the considered problem, $\mathbf{S}^{\text{LC,T}}$ must satisfy two basic properties:

- 1) *Symmetry*. Due to reciprocity, we expect

$$(\mathbf{S}^{\text{LC,T}})^T = \mathbf{S}^{\text{LC,T}}. \quad (18)$$

- 2) *Unitarity*. Due to the absence of loss and gain, we expect

$$(\mathbf{S}^{\text{LC,T}})^\dagger \mathbf{S}^{\text{LC,T}} = \mathbf{I}_5. \quad (19)$$

Verifying that these two expectations are met constitutes the first two sanity checks, which are easily passed by the form of \mathbf{S}^{LC} defined in Eq. (12).

Furthermore, it is well-established that the impedance matrix of an ideal T network with impedances Z_1 , Z_2 and Z_3 , as sketched in Fig. 2A, is given by

$$\mathbf{Z}^T = \begin{bmatrix} Z_1 + Z_3 & Z_3 \\ Z_3 & Z_2 + Z_3 \end{bmatrix} \in \mathbb{C}^{2 \times 2}. \quad (20)$$

This ideal T network corresponds to terminating ports 3, 4 and 5 of our 5-port network (sketched in Fig. 2B) with load impedances Z_1 , Z_2 and Z_3 . Our third sanity check hence consists in verifying that based on the form of $\mathbf{S}^{\text{LC,T}}$ defined in Eq. (12) we recover the well-established \mathbf{Z}^T from Eq. (20) for random complex-valued choices of the values of Z_1 , Z_2 and Z_3 .

Since our 5-port network is characterized by a scattering matrix that cannot be converted to an impedance matrix, we first determine the reflection coefficients of the three individual load impedances using $r_i = (Z_i - Z_0)/(Z_i + Z_0)$. Then, we define $\mathbf{r} = \text{diag}([r_1, r_2, r_3])$ and evaluate

$$\mathbf{S}^T = \mathbf{S}_{\bar{S}\bar{S}}^{\text{LC,T}} + \mathbf{S}_{\bar{S}C}^{\text{LC,T}} \left((\text{diag}(\mathbf{r}))^{-1} - \mathbf{S}_{CC}^{\text{LC,T}} \right)^{-1} \mathbf{S}_{C\bar{S}}^{\text{LC,T}}, \quad (21)$$

where $\bar{S} = \{1, 2\}$ and $C = \{3, 4, 5\}$. Finally, we confirm that $Z_0(\mathbf{I}_2 + \mathbf{S}^T)(\mathbf{I}_2 - \mathbf{S}^T)^{-1}$ equals \mathbf{Z}^T obtained via Eq. (20).

The form of $\mathbf{S}^{\text{LC,T}}$ defined in Eq. (12) passes all three sanity checks.

ACKNOWLEDGMENT

The author acknowledges stimulating discussions with M. Nerini, H. Prod'homme, and A. Shaham.

REFERENCES

- [1] P. del Hougne, "Physics-compliant diagonal representation of beyond-diagonal RIS," *arXiv:2403.17222*, 2024.
- [2] L. Subrt and P. Pechac, "Intelligent walls as autonomous parts of smart indoor environments," *IET Commun.*, vol. 6, no. 8, pp. 1004–1010, May 2012.
- [3] C. Liaskos, S. Nie, A. I. Tsioliaridou, A. Pitsillides, S. Ioannidis, and I. F. Akyildiz, "A new wireless communication paradigm through software-controlled metasurfaces," *IEEE Commun. Mag.*, vol. 56, no. 9, pp. 162–169, Sep. 2018.
- [4] P. del Hougne, M. Fink, and G. Lerosey, "Optimally diverse communication channels in disordered environments with tuned randomness," *Nat. Electron.*, vol. 2, no. 1, pp. 36–41, 2019.
- [5] M. Di Renzo, A. Zappone, M. Debbah, M.-S. Alouini, C. Yuen, J. De Rosny, and S. Tretyakov, "Smart radio environments empowered by reconfigurable intelligent surfaces: How it works, state of research, and the road ahead," *IEEE J. Sel. Areas Commun.*, vol. 38, no. 11, pp. 2450–2525, 2020.
- [6] G. C. Alexandropoulos, N. Shlezinger, and P. del Hougne, "Reconfigurable intelligent surfaces for rich scattering wireless communications: Recent experiments, challenges, and opportunities," *IEEE Commun. Mag.*, vol. 59, no. 6, pp. 28–34, 2021.
- [7] S. Shen, B. Clerckx, and R. Murch, "Modeling and architecture design of reconfigurable intelligent surfaces using scattering parameter network analysis," *IEEE Trans. Wirel. Commun.*, vol. 21, no. 2, pp. 1229–1243, 2021.

- [8] H. Li, S. Shen, M. Nerini, and B. Clerckx, "Reconfigurable intelligent surfaces 2.0: Beyond diagonal phase shift matrices," *IEEE Commun. Mag.*, vol. 62, no. 3, pp. 102–108, 2024.
- [9] K. Shastri and F. Monticone, "Nonlocal flat optics," *Nat. Photonics*, vol. 17, no. 1, pp. 36–47, 2023.
- [10] Y. Chen, M. A. Abouelatta, K. Wang, M. Kadic, and M. Wegener, "Nonlocal cable-network metamaterials," *Adv. Mater.*, vol. 35, no. 15, p. 2209988, 2023.
- [11] J. Sol, M. Röntgen, and P. del Hougne, "Covert scattering control in metamaterials with non-locally encoded hidden symmetry," *Adv. Mater.*, vol. 36, no. 11, p. 2303891, 2024.
- [12] J. Sol, D. R. Smith, and P. del Hougne, "Meta-programmable analog differentiator," *Nat. Commun.*, vol. 13, no. 1, p. 1713, 2022.
- [13] J. Sol, A. Alhulaymi, A. D. Stone, and P. del Hougne, "Reflectionless programmable signal routers," *Sci. Adv.*, vol. 9, no. 4, p. eadf0323, 2023.
- [14] F. T. Faul, L. Cronier, A. Alhulaymi, A. D. Stone, and P. del Hougne, "Agile free-form signal filtering with a chaotic-cavity-backed non-local programmable metasurface," *arXiv:2407.00054*, 2024.
- [15] E. Denicke, M. Henning, H. Rabe, and B. Geck, "The application of multiport theory for MIMO RFID backscatter channel measurements," *Proc. EuMC*, pp. 522–525, 2012.
- [16] P. del Hougne, "Virtual VNA 2.0: Ambiguity-free scattering matrix estimation by terminating inaccessible ports with tunable and coupled loads," *arXiv:2409.10977*, 2024.
- [17] A. Rabault, L. Le Magoarou, J. Sol, G. C. Alexandropoulos, N. Shlezinger, H. V. Poor, and P. del Hougne, "On the tacit linearity assumption in common cascaded models of RIS-parametrized wireless channels," *IEEE Trans. Wirel. Commun.*, vol. 23, no. 8, pp. 10001–10014, 2024.
- [18] R. Faqiri, C. Saigre-Tardif, G. C. Alexandropoulos, N. Shlezinger, M. F. Imani, and P. del Hougne, "PhysFad: Physics-based end-to-end channel modeling of RIS-parametrized environments with adjustable fading," *IEEE Trans. Wirel. Commun.*, vol. 22, no. 1, pp. 580–595, 2022.
- [19] J. Sol, H. Prod'homme, L. Le Magoarou, and P. del Hougne, "Experimentally realized physical-model-based frugal wave control in metasurface-programmable complex media," *Nat. Commun.*, vol. 15, no. 1, p. 2841, 2024.
- [20] H. Prod'homme and P. del Hougne, "Efficient computation of physics-compliant channel realizations for (rich-scattering) RIS-parametrized radio environments," *IEEE Commun. Lett.*, vol. 27, no. 12, pp. 3375–3379, 2023.
- [21] C. Seguinot, P. Kennis, J.-F. Legier, F. Huret, E. Paleczny, and L. Hayden, "Multimode TRL: a new concept in microwave measurements: theory and experimental verification," *IEEE Trans. Microw. Theory Techn.*, vol. 46, no. 5, pp. 536–542, 1998.
- [22] M. T. Ivrlač and J. A. Nossek, "Toward a circuit theory of communication," *IEEE Trans. Circuits Syst. I: Regul. Pap.*, vol. 57, no. 7, pp. 1663–1683, 2010.
- [23] —, "The multiport communication theory," *IEEE Circuits Syst. Mag.*, vol. 14, no. 3, pp. 27–44, 2014.
- [24] G. Gradoni and M. Di Renzo, "End-to-end mutual coupling aware communication model for reconfigurable intelligent surfaces: An electromagnetic-compliant approach based on mutual impedances," *IEEE Wirel. Commun. Lett.*, vol. 10, no. 5, pp. 938–942, 2021.
- [25] Z. Zhang, J. W. Zhang, J. W. Wu, J. C. Liang, Z. X. Wang, Q. Cheng, Q. S. Cheng, T. J. Cui, H. Q. Yang, G. B. Liu, and S. R. Wang, "Macromodeling of reconfigurable intelligent surface based on microwave network theory," *IEEE Trans. Antennas Propag.*, vol. 70, no. 10, pp. 8707–8717, 2022.
- [26] D. Badheka, J. Sapis, S. R. Khosravirad, and H. Viswanathan, "Accurate modeling of intelligent reflecting surface for communication systems," *IEEE Trans. Wirel. Commun.*, vol. 22, no. 9, pp. 5871–5883, 2023.
- [27] P. Mursia, S. Phang, V. Sciancalepore, G. Gradoni, and M. D. Renzo, "SARIS: Scattering aware reconfigurable intelligent surface model and optimization for complex propagation channels," *IEEE Wirel. Commun. Lett.*, vol. 12, no. 11, pp. 1921–1925, 2023.
- [28] J. Tapie, H. Prod'homme, M. F. Imani, and P. del Hougne, "Systematic physics-compliant analysis of over-the-air channel equalization in RIS-parametrized wireless networks-on-chip," *IEEE J. Sel. Areas Commun.*, vol. 42, no. 8, pp. 2026–2038, 2024.
- [29] M. Akrouf, F. Bellili, A. Mezghani, and J. A. Nossek, "Physically consistent models for intelligent reflective surface-assisted communications under mutual coupling and element size constraint," *Proc. ACSSC*, pp. 1589–1594, 2023.
- [30] P. del Hougne, "Virtual VNA: Minimal-ambiguity scattering matrix estimation with load-tunable ports," *arXiv:2403.08074*, 2024.
- [31] J. A. Nossek, D. Semmler, M. Joham, and W. Utschick, "Physically consistent modeling of wireless links with reconfigurable intelligent surfaces using multiport network analysis," *IEEE Wirel. Commun. Lett.*, vol. 13, no. 8, pp. 2240–2244, 2024.
- [32] K. Konno, S. Terranova, Q. Chen, and G. Gradoni, "Generalised impedance model of wireless links assisted by reconfigurable intelligent surfaces," *IEEE Trans. Antennas Propag.*, 2024.
- [33] M. Nerini, S. Shen, H. Li, M. D. Renzo, and B. Clerckx, "A universal framework for multiport network analysis of reconfigurable intelligent surfaces," *IEEE Trans. Wirel. Commun.*, 2024.
- [34] O. Franek, "Electromagnetics-based RIS channel model with near-field accuracy improvement," *Proc. EuCAP*, pp. 1–5, 2024.
- [35] A. D. Kuznetsov, J. Holopainen, and V. Viikari, "Predicting the bistatic scattering of a multiport loaded structure under arbitrary excitation: The S-parameters approach," *IEEE Trans. Antennas Propag.*, vol. 72, no. 8, pp. 6691–6701, 2024.
- [36] A. Abrardo, A. Toccafondi, and M. Di Renzo, "Design of reconfigurable intelligent surfaces by using s-parameter multiport network theory – optimization and full-wave validation," *IEEE Trans. Wirel. Commun.*, 2024.
- [37] H. Li, S. Shen, M. Nerini, M. Di Renzo, and B. Clerckx, "Beyond diagonal reconfigurable intelligent surfaces with mutual coupling: Modeling and optimization," *IEEE Commun. Lett.*, vol. 28, no. 4, pp. 937–941, 2024.
- [38] D. King, "The measurement and interpretation of antenna scattering," *Proc. IRE*, vol. 37, no. 7, pp. 770–777, 1949.
- [39] R. C. Hansen, "Relationships between antennas as scatterers and as radiators," *Proc. IEEE*, vol. 77, no. 5, pp. 659–662, 1989.
- [40] R. Hansen, "Antenna mode and structural mode RCS: dipole," *Microw. Opt. Technol. Lett.*, vol. 3, no. 1, pp. 6–10, 1990.
- [41] R. Redheffer, "Inequalities for a Matrix Riccati Equation," *J. Math. Mech.*, vol. 8, no. 3, pp. 349–367, 1959.
- [42] T. S. Chu and T. Itoh, "Generalized scattering matrix method for analysis of cascaded and offset microstrip step discontinuities," *IEEE Trans. Microw. Theory Techn.*, vol. 34, no. 2, pp. 280–284, 1986.
- [43] P. Overfelt and D. White, "Alternate forms of the generalized composite scattering matrix," *IEEE Trans. Microw. Theory Techn.*, vol. 37, no. 8, pp. 1267–1268, 1989.
- [44] H. Prod'homme and P. del Hougne, "Efficient and updatable evaluation of arbitrarily complex connections between multi-port networks," *in preparation*, 2024.
- [45] S. Shen and R. D. Murch, "Impedance matching for compact multiple antenna systems in random RF fields," *IEEE Trans. Antennas Propag.*, vol. 64, no. 2, pp. 820–825, 2016.
- [46] MACOM. MADP-000907-14020x. [Online]. Available: <https://cdn.macom.com/datasheets/MADP-000907-14020x.pdf>
- [47] H. Li, S. Shen, Y. Zhang, and B. Clerckx, "Channel estimation and beamforming for beyond diagonal reconfigurable intelligent surfaces," *arXiv:2403.18087*, 2024.
- [48] A. L. de Almeida, B. Sokal, H. Li, and B. Clerckx, "Channel estimation for beyond diagonal RIS via tensor decomposition," *arXiv:2407.20402*, 2024.
- [49] J. Sol, L. Le Magoarou, and P. del Hougne, "Optimal blind focusing on perturbation-inducing targets in sub-unitary complex media," *Laser Photonics Rev.*, p. 2400619, 2024.
- [50] D. M. Pozar, *Microwave Engineering*, 4th ed., Hoboken, NJ: Wiley, 2011.